

26 **Address correspondence to:**

27 Laura Herrero, PhD

28 Department of Biochemistry and Molecular Biology, IBUB

29 School of Pharmacy

30 University of Barcelona

31 Av. Diagonal, 643

32 E-08028 Barcelona, Spain

33 Tel: (+34) 934 024 522

34 Fax: (+34) 934 024 520

35 Email: lherrero@ub.edu

36

37 **Running head**

38 Fatty acid oxidation in adipocytes and macrophages

39

40 **Conflict of interest statement**

41 All authors declare no conflict of interest to disclose.

42

43

44 **ABSTRACT**

45 Lipid overload in obesity and type 2 diabetes is associated with adipocyte dysfunction,
46 inflammation, macrophage infiltration and decreased fatty acid oxidation (FAO). Here
47 we report that the expression of carnitine palmitoyltransferase 1A (CPT1A), the rate-
48 limiting enzyme in mitochondrial FAO, is higher in human adipose tissue macrophages
49 than in adipocytes and that it is differentially expressed in visceral vs. subcutaneous
50 adipose tissue both in an obese and a type 2 diabetes cohort. These observations led us
51 to further investigate the potential role of CPT1A in adipocytes and macrophages. We
52 expressed CPT1AM, a permanently active mutant form of CPT1A, in 3T3-L1 CAR Δ 1
53 adipocytes and RAW 264.7 macrophages through adenoviral infection. Enhanced FAO
54 in palmitate-incubated adipocytes and macrophages reduced triglyceride content and
55 inflammation, improved insulin sensitivity in adipocytes and reduced ER stress and
56 ROS damage in macrophages. We conclude that increasing FAO in adipocytes and
57 macrophages improves palmitate-induced derangements. This indicates that enhancing
58 FAO in metabolically relevant cells such as adipocytes and macrophages may be a
59 promising strategy for the treatment of chronic inflammatory pathologies such as
60 obesity and type 2 diabetes.

61

62 **Keywords**

63 Obesity, type 2 diabetes, adipocytes, macrophages, inflammation, fatty acid oxidation,
64 CPT1.

65

66 **Abbreviations**

67 Ad, adenovirus; AGPAT5, 1-acylglycerol-3-phosphate O-acyltransferase 5; BCL2, B-
68 cell CLL/lymphoma 2; CD163, macrophage and monocyte marker; CHOP, C/EBP
69 homologous protein; CPT1A, carnitine palmitoyltransferase 1A; CPT1AM, carnitine
70 palmitoyltransferase 1A (permanently active mutant form); EDEM, ER degradation
71 enhancing α -mannosidase-like protein; ER, endoplasmic reticulum; FA, fatty acids;
72 FAO, fatty acid oxidation; GFP, green fluorescent protein; IL-1 β , interleukin-1 β ; IL-6,
73 interleukin-6; IRbeta, insulin receptor beta; MCP-1, monocyte chemoattractant protein-
74 1; moi, multiplicity of infection; PDI, protein disulfide isomerase; ROS, reactive
75 oxygen species; SAT, subcutaneous adipose tissue; SREBF1, Sterol regulatory element
76 binding transcription factor 1; SVF, stromal-vascular fraction; TLR-4, toll-like receptor-
77 4; VAT, visceral adipose tissue; WAT, white adipose tissue.

78

79

80

81

82 INTRODUCTION

83 Obesity has reached epidemic proportions worldwide, leading to severe
84 associated pathologies such as insulin resistance, type 2 diabetes (T2D), cardiovascular
85 disease, Alzheimer's disease, hypertension, hypercholesterolemia, hypertriglyceridemia,
86 non-alcoholic fatty liver disease (NAFLD), arthritis, asthma, and certain forms of
87 cancer (12).

88 Over the last two decades adipose tissue has gained crucial importance in the
89 mechanisms involved in obesity-related disorders. The energy-storing white adipose
90 tissue (WAT) is well vascularized and contains adipocytes, connective tissue and
91 numerous immune cells such as macrophages, T and B cells, mast cells and neutrophils
92 that infiltrate and increase their presence during obesity (22). Macrophages were the
93 first immune cells reported to participate in obesity-induced insulin resistance (56). This
94 highlights their pathological role in adipose tissue in addition to their traditional
95 involvement in tissue repair and in response to dead and dying adipocytes (5, 14). Fat is
96 an active endocrine tissue that secretes hormones such as leptin, adiponectin or resistin
97 and inflammatory cytokines such as TNF- α , IL-6, IL-1 β , etc. in response to several
98 stimuli. It is therefore a complex organ controlling energy expenditure, appetite, insulin
99 sensitivity, endocrine and reproductive functions, inflammation and immunity (53).

100 The pathophysiology of obesity-induced insulin resistance has been attributed to
101 ectopic fat deposition (39), increased inflammation and ER stress (16, 42), adipose
102 tissue hypoxia (15) and mitochondrial dysfunction (32), and impaired adipocyte
103 expansion and angiogenesis (50, 51, 54). In obesity, fatty acids (FA) together with other
104 stimuli such as ceramide, various PKC isoforms, proinflammatory cytokines and ROS
105 and ER stresses activate JNK, NF- κ B, RAGE and TLR pathways both in adipocytes and
106 macrophages triggering inflammation and insulin resistance (43).

107 Strenuous efforts are being made by the research community to elucidate the
108 mechanisms involved in the pathophysiology of obesity-related disorders. However, an
109 alternative strategy could be to act upstream by preventing the accumulation of lipids
110 and the progression of obesity. In addition to reducing caloric intake, a potential
111 effective approach to combat obesity would be to increase energy expenditure in key
112 metabolic organs, such as adipose tissue. Obese individuals and those with T2D are
113 known to have lower fatty acid oxidation (FAO) rates and lower electron transport chain
114 activity in muscle (17, 19, 37) together with higher glycolytic capacities and enhanced
115 cellular FA uptake compared to non-obese and non-diabetic individuals (44). Thus, any
116 strategy able to eliminate the excess of lipids found in obesity could be beneficial for
117 health. Lipid levels can be reduced by inhibiting synthesis, transport or by increasing
118 oxidation: here we focus on the latter.

119 Malonyl-CoA, derived from glucose metabolism and the first intermediate in
120 lipogenesis, regulates FAO by inhibiting carnitine palmitoyltransferase 1 (CPT1). This
121 makes CPT1 the rate-limiting step in mitochondrial FA β -oxidation. Thus, in high-
122 energy conditions malonyl-CoA inhibits oxidation diverting FAs fate into TG
123 accumulation. There are three CPT1 isoforms, with differential tissue expression:
124 CPT1A (liver, kidney, intestine, pancreas, ovary and mouse and human WAT), CPT1B
125 (brown adipose tissue, skeletal muscle, heart and rat and human WAT), and CPT1C
126 (brain and testis) (2, 36). The fact that CPT1 controls FAO makes it a very attractive
127 target to reduce lipid levels and fight against obesity and T2D. In spite of their excess
128 fat, obese individuals have reduced visceral WAT CPT1 mRNA and protein levels (20).
129 This prompted our group and others to overexpress CPT1 in liver (26, 30, 46), muscle
130 (4, 33, 41), and white adipocytes (9), which led to a decrease in TG content and an
131 improvement in insulin sensitivity.

132 Here we showed that CPT1A expression was higher in human adipose tissue
133 macrophages than in mature adipocytes and that it was differentially expressed in
134 visceral *vs.* subcutaneous adipose tissue. To further investigate the role of CPT1A in
135 both adipocytes and macrophages we used a permanently active mutant form of
136 CPT1A, CPT1AM, which is insensitive to its inhibitor malonyl-CoA (27), to achieve
137 continuous oxidation of lipids. When cells were incubated with palmitate to mimic
138 obesity, CPT1AM restored most of the palmitate-induced imbalances. An increase in
139 FAO in adipocytes and macrophages reduced TG content and inflammatory levels,
140 improved insulin sensitivity in adipocytes, and reduced endoplasmic reticulum (ER)
141 stress and ROS damage in macrophages.

142

143 **MATERIALS AND METHODS**

144 *Human cohorts*

145 *Selection of patients*

146 Adipose tissue was selected from an adipose tissue biobank collection of the University
147 Hospital Joan XXII (Tarragona, Spain). All subjects were of Caucasian origin and
148 reported that their body weight had been stable for at least 3 months before the study.
149 They had no systemic disease other than obesity or T2D, and all had been free of any
150 infections in the previous month before the study. Liver and renal diseases were
151 specifically excluded by biochemical work-up. Appropriate Institutional Review Board
152 approval and adequate biobank informed consent was obtained from all participants.
153 Bio-banking samples included plasma, total and fractionated adipose tissue from
154 subcutaneous and visceral origin. All patients had fasted overnight before collection of
155 blood and adipose tissue samples. Visceral adipose tissue (VAT) and subcutaneous
156 adipose tissue (SAT) samples were obtained during surgical procedures that included
157 laparoscopic surgery for hiatus hernia repair or cholecystectomy. Samples were selected
158 according stratification by age, gender and BMI and grouped into two cohorts:
159 Obesity cohort. Subjects were classified by BMI according to the World Health
160 Organization criteria (WHO, 2000). The study included 19 lean, 28 overweight, and 15
161 obese non-diabetic subjects, matched for age and gender (Table 1).
162 Type 2 diabetes cohort. Patients were classified as having T2D according to the
163 American Diabetes Association criteria (1997). Variability in metabolic control was
164 assessed by stable glycated hemoglobin A1c (HbA1c) values during the previous 6
165 months. Gathering these criteria, there were 11 T2D subjects. As a control group, we
166 selected 36 subjects without diabetes from the obesity cohort, matched for age, BMI and
167 gender (Table 2). No patient was being treated with thiazolidinedione.

168

169 *Anthropometric measurements*

170 Height was measured to the nearest 0.5 cm and body weight to the nearest 0.1 kg. BMI
171 was calculated as weight (kilograms) divided by height (meters) squared. Waist
172 circumference was measured midway between the lowest rib margin and the iliac crest.

173

174 *Collection and processing of human samples*

175 Samples from VAT (visceral adipose tissue, omental) and SAT (subcutaneous adipose
176 tissue, anterior abdominal wall) from the same individual were obtained during
177 abdominal elective surgical procedures (cholecystectomy or surgery for abdominal
178 hernia). All patients had fasted overnight, at least 12 hours before surgical procedure.
179 Blood samples were collected before the surgical procedure from the antecubital vein,
180 20 ml of blood with EDTA (1mg/ml) and 10 ml of blood in silicone tubes. 15 ml of
181 collected blood was used for the separation of plasma. Plasma samples were stored at -
182 80°C until analytical measurements were performed. 5 ml of blood with EDTA was
183 used for the determination of HbA1c. Adipose tissue samples were collected, washed in
184 PBS, immediately frozen in liquid N₂ and stored at -80°C.

185

186 *Adipose tissue fractionation*

187 Adipose tissue biopsies were immediately processed. The adipose tissue was finely
188 diced into small pieces (10-30 mg), washed in PBS and incubated in Medium 199 (Life
189 Technologies) supplemented with 4% BSA plus 2 mg/ml of collagenase Type I (Sigma)
190 for 1 h in a shaking water bath at 37°C. After digestion, mature adipocytes (ADI) were
191 separated from tissue matrix by filtration through a 200 µm mesh fabric (Spectrum
192 Laboratories). The filtrated solution was centrifuged for 5 min at 1500xg. The mature

193 adipocytes were removed from the top layer and the SVF cells remained in the pellet.
194 Cells were washed 4 times in PBS and processed for RNA and protein extraction.

195

196 *Analytical methods*

197 Glucose, cholesterol and TG plasma levels were determined in an auto-analyser
198 (Hitachi 737, Boehringer Mannheim) using the standard enzyme methods. High-density
199 lipoprotein (HDL) cholesterol was quantified after precipitation with polyethylene
200 glycol at room temperature (PEG-6000). Plasma insulin was determined by
201 radioimmunoassay (Coat-A-Count insulin; Diagnostic Products Corp.). Non-esterified
202 Free Fat Acid (NEFA) serum levels were determined in an autoanalyser (Advia 1200,
203 Siemens AG) using an enzymatic method developed by Wako Chemicals. Plasma
204 glycerol levels were analyzed by using a free glycerol determination kit, a quantitative
205 enzymatic determination assay (Sigma-Aldrich Corp.). Intra- and interassay CV were
206 less than 6% and less than 9.1%, respectively. The degree of insulin resistance was
207 determined by the homeostasis model assessment (HOMA), as $[\text{glucose (mmol/l)} \times$
208 $\text{insulin (mIU/l)}] / 22.5$ (24).

209

210 *Immunohistochemistry*

211 Five-micron sections of formalin-fixed paraffin-embedded adipose tissue were
212 deparaffinised and rehydrated prior to antigen unmasking by boiling in 1mM EDTA,
213 pH 8. Sections were blocked in normal serum and incubated overnight with rabbit anti-
214 CPT1A (Sigma-Aldrich) at 1:50 dilution. Secondary antibody staining was performed
215 using the VECTASTAIN ABC kit (Vector Laboratories, Inc.) and detected with
216 diaminobenzidine (DAB, Vector Laboratories, Inc.). Sections were counterstained with
217 hematoxylin prior to dehydration and coverslip placement, and examined under a Nikon

218 Eclipse 90i microscope. As a negative control, the procedure was performed in the
219 absence of primary antibody.

220

221 *Immunofluorescence*

222 Five-micron sections of formalin-fixed paraffin-embedded adipose tissue were blocked
223 in normal serum and incubated overnight with rabbit anti-CPT1A antibody (Sigma-
224 Aldrich) at 1:50 dilution, and with mouse anti-CD68 (Santa Cruz Biotechnology, Inc.)
225 at 1:50 dilution, washed, and visualized using Alexa Fluor 546 goat anti-rabbit, and
226 Alexa Fluor 488 goat anti-mouse antibodies, respectively (1:500; Molecular Probes
227 Inc.). The slides were counterstained with DAPI (4,6-diamidino-2-phenylindole) to
228 reveal nuclei and were examined under a Nikon Eclipse 90i fluorescent microscope. As
229 a negative control, the assay was performed in the absence of primary antibody.

230

231 *Materials*

232 Sodium palmitate, sodium oleate, BSA and L-carnitine hydrochloride were purchased
233 from Sigma Aldrich. DMEM, FBS and Penicillin/Streptomycin mixture were purchased
234 from Life Technologies.

235

236 *Cell culture*

237 Murine 3T3-L1 CARΔ1 preadipocytes, kindly given by Dr. Orlicky (Department of
238 Pathology, UCHSC at Fitzsimons, Aurora, CO, USA), were cultured and differentiated
239 into mature adipocytes following the published protocol (31). Mature adipocytes were
240 used for experiments at day 8 post-differentiation. Murine RAW 264.7 macrophages
241 were obtained from ATCC and were maintained in DMEM supplemented with 10%
242 heat-inactivated FBS and 1% penicillin/streptomycin mixture. Simpson-Golabi-Behmel

243 Syndrome (SGBS) human cells were cultured and differentiated to adipocytes as
244 previously described (55).

245

246 *Adenovirus (Ad) infection*

247 At day 8 of differentiation, 3T3-L1 CAR Δ 1 cells were infected with AdGFP (100 moi)
248 and AdCPT1AM (13) (100 moi) for 24 h in serum-free DMEM and then the medium
249 was replaced with complete DMEM for additional 24 h. RAW 264.7 macrophages were
250 infected with AdGFP (100 moi) and AdCPT1AM (100 moi) for 2 h in serum-free
251 DMEM and then replaced with complete medium for additional 72 h. The adenovirus
252 infection efficiency was assessed in AdGFP-infected cells (Figure 3A and B). The same
253 batch of adenoviruses stored in 50 μ l aliquots was used throughout the experiments.

254

255 *Fatty acid (FA) treatment*

256 Sodium palmitate was conjugated with FA-free BSA in a 5:1 ratio to yield a stock
257 solution of 2.5mM (41). Cells were incubated with 0.3 mM or 1 mM of this solution for
258 24 h (3T3-L1 CAR Δ 1 adipocytes) or 0.3 mM, 0.5 mM or 0.75 mM for 24, 8 or 18 h
259 (RAW 264.7 macrophages), respectively.

260

261 *Adipocyte and macrophage viability*

262 3T3-L1 CAR Δ 1 adipocytes and RAW 264.7 macrophages were infected as previously
263 described and incubated for 24h with 1mM or 0.3mM palmitate, respectively. Cells
264 were washed twice with PBS and lifted from the surface with trypsin followed by 2 min
265 incubation at 37°C. Trypsinization was stopped with 10% FBS containing media and
266 equal volumes of cell suspension were mixed with 0.4% Trypan blue staining. Trypan
267 blue positive and negative cells were counted using a Neubauer chamber for adipocytes

268 and Countess Automated Cell Counter (Invitrogen) for macrophages. Percentage of
269 viability was determined normalizing viable cells of each group to viable cells of BSA
270 GFP group. Statistical significance was assessed using two-way Anova analysis of three
271 individual experiments (* p<0.05).

272

273 *CPT1 activity*

274 Mitochondria-enriched fractions were obtained from cell culture grown in 10-cm²
275 dishes and CPT1 activity was measured by a radiometric method as described (13).

276

277 *Fatty acid oxidation*

278 Total oleate oxidation was measured in 3T3-L1 CARΔ1 adipocytes and RAW 264.7
279 macrophages grown in 25-cm² flasks, differentiated, and infected as described above.
280 The day of the assay cells were washed in KRBH 0.1% BSA, preincubated at 37°C for
281 30 min in KRBH 1% BSA, and washed again in KRBH 0.1% BSA. Cells were then
282 incubated for 3 h (3T3-L1 CARΔ1 adipocytes) or 2 h (RAW 264.7 macrophages) at
283 37°C with fresh KRBH containing 11 mM glucose, 0.8 mM carnitine plus 0.2 mM [1-
284 ¹⁴C] oleate (Perkin Elmer). Oxidation was measured as described (30). The scintillation
285 values were normalized to the protein content of each flask.

286

287 *TG content*

288 Cells were grown in 12-well plates, differentiated and infected as described above.
289 After 24 h (3T3-L1 CARΔ1 adipocytes) or 18 h (RAW 264.7 macrophages) of FA
290 treatment, cells were collected for lipid extraction following Gesta *et al* protocol (10)
291 with minor modifications: after cell lysis with 0.1% SDS, 1/2/0.12 (v/v/v)
292 methanol/chloroform/0.5M KCl solution was added, the two phases were separated by

293 centrifugation and the upper phase was dried with N₂. Finally, lipids were resuspended
294 in 100% isopropanol and TG were quantified using TG Triglyceride kit (Sigma),
295 according to the manufacturer's instructions. Protein concentrations were used to
296 normalize sample values.

297

298 *Oil Red O staining*

299 RAW 264.7 macrophages grown on coverslips were infected as described above and
300 incubated with 0.75 mM of palmitate for 18 hours. After this time, cells were rinsed
301 twice with PBS, fixed in 10% paraformaldehyde for 30 minutes at room temperature
302 and washed again with PBS. Then, cells were rinsed with 60% isopropanol for 5 min to
303 facilitate the staining of neutral lipids and stained with filtered Oil Red O working
304 solution (0.3 % Oil Red O in isopropanol) for 15 min. After several washes with
305 distilled water the coverslips were removed and mounted on a drop of mount medium.
306 The intracellular lipid vesicles stained with Oil Red O were identified by their bright red
307 color under the microscope.

308

309 *Analysis of intracellular protein oxidation*

310 RAW 264.7 macrophages were cultured in 12-well plates and infected as described
311 before. After FA treatment, cell extracts were prepared and analyzed for protein
312 oxidative modifications (*i.e.* carbonyl group content) with OxyBlot Protein Oxidation
313 Detection kit (Millipore), following the manufacturer's instructions.

314

315 *Western blot analysis*

316 3T3-L1 CARΔ1 adipocytes and RAW 264.7 macrophages were cultured in 12-well
317 plates, differentiated, and infected as described above. Cells were collected in lysis

318 buffer (RIPA) and protein concentration was determined using the BCA protein assay
319 kit (Thermoscientific). Equal amount of protein from whole cell lysates was resolved by
320 8% SDS-PAGE and transferred to PVDF membranes (Millipore). Signal detection was
321 carried out with the ECL immunoblotting detection system (GE Healthcare) and the
322 results were quantitatively analyzed using Image Quant LAS4000 Mini (GE
323 Healthcare). The following antibodies were used: CPT1A (1/6,000; (13)), β -actin (I-19)
324 (1/4,000; Santa Cruz), Akt and pAkt (Ser⁴⁷³) (1/1,000; Cell Signaling), CHOP (GADD
325 153; 1/200; Santa Cruz) and IRbeta (1/1,000; Santa Cruz). Human fat tissue was
326 homogenized in RIPA buffer as previously described (34). Protein extracts (10-20 μ g)
327 were loaded, resolved on 10% SDS-PAGE and transferred to Hybond ECL
328 nitrocellulose membranes. Membranes were stained with 0.15% Ponceau red (Sigma-
329 Aldrich) to ensure equal loading after transfer and then blocked with 5% (w/v) BSA in
330 TBS buffer with 0.1% Tween 20. Immunoblotting was performed with 1:2000 goat
331 anti-human CPT1A (Abcam). Blots were incubated with the appropriate IgG-HRP-
332 conjugated secondary antibody. Immunoreactive bands were visualized with an ECL-
333 plus reagent kit (GE Healthcare). Optical densities of the immunoreactive bands were
334 measured using Image J analysis software.

335

336 *Analysis of mRNA expression by quantitative real-time PCR*

337 Total RNA was extracted from cultured cells grown in 12-well plates using Illustr
338 MiniRNA Spin kit (GE Healthcare) and cDNA was obtained using Transcriptor First
339 Strand cDNA Synthesis kit (Roche). Quantitative real-time PCR was performed using
340 SYBR Green PCR Master Mix Reagent Kit (Life Technologies). Levels of mRNA were
341 normalized to those of β -actin and expressed as fold change. Forward/reverse primers
342 for several used genes (other sequences are available upon request):

	FORWARD	REVERSE
β-ACTIN	5'- AGGTGACAGCATTGCTTCTG- 3'	5'- GCTGCCTCAACACCTCAAC-3'
CHOP	5'-CCCTGCCTTTTACCTTGG- 3'	5'-CCGCTCGTTCTCCTGCTC- 3'
CPT1A*	5'- GCAGCAGATGCAGCAGATCC- 3'	5'-TCAGGATCCTCCTCTCTGTATCCC3'
EDEM	5'-AAGCCCTCTGGAACCTGCG- 3'	5'-AACCCAATGGCCTGTCTGG- 3'
GRP78	5'-ACTTGGGGACCACCTATTCCT- 3'	5'-ATCGCCAATCAGACGCTCC- 3'
IL-1β	5'- GCCCATCCTCTGTGACTCAT- 3'	5'- AGGCCACAGGTATTTTGTGTCG- 3'
MCP-1	5'- TCCCAATGAGTAGGCTGGAG-3'	5'- AAGTGCTTGAGGTGGTTGTG- 3'
PDI	5'-ACCTGCTGGTGGAGTTCTATG- 3'	5'-CGGCAGCTTTGGCATACT- 3'
TLR-4	5'- GGACTCTGATCATGGCACTG- 3'	5'- CTGATCCATGCATTGGTAGGT- 3'
TNF-α	5'-ACGGCATGGATCTCAAAAGAC-3'	5'-AGATAGCAAATCGGCTGAACG- 3'

344 * Recognizes both CPT1A and CPT1AM

345 400-500mg frozen human adipose tissue was homogenized with an Ultra-Turrax
346 8 (Ika). Total RNA from adipose biopsies, stromal-vascular fractions (SVF) and isolated
347 adipocytes were extracted by using RNeasy Lipid Tissue Midi Kit (QIAGEN Science)
348 following the manufacturer's instructions and total RNA was treated with 55 U RNase-
349 free DNase (QIAGEN) to avoid contamination with genomic DNA. Between 0.2 and 1
350 µg of total RNA was reverse-transcribed to cDNA using TaqMan Reverse Transcription
351 reagents (Applied Biosystems), and subsequently diluted with nuclease-free water
352 (Sigma) to 20 ng/µl cDNA. For adipose tissue gene expression analysis a real-time
353 quantitative PCR was performed, with duplicates, on a 7900HT Fast Real-Time PCR
354 System using commercial Taqman Assays (Applied Biosystems). SDS software 2.3 and
355 RQ Manager 1.2 (Applied Biosystems) were used to analyse the results with the
356 comparative threshold cycle (Ct) method ($2^{\Delta\Delta C_t}$). C_t values for each sample were
357 normalized with an optimal reference gene (cyclophilin), after testing three additional

358 housekeeping genes: β -actin and RNA 18S. A panel of genes involved in the adipocyte
 359 differentiation and metabolism was selected in the study of CPT1A gene expression:

GEN SIMBOL	GENE DENOMINATION	ASSAI ID
ACC1	(acetyl-coenzyme carboxylase 1) ACACA	Hs00167385_m1
PCK2	(phosphoenolpyruvate carboxykinase 2)	Hs00388934_m1
PPAR α	(peroxisome proliferator-activated receptor α)	Hs00231882_m1
PPAR γ	(peroxisome proliferator-activated receptor λ)	Hs00234592_m1
AGPAT3	(1-acyl-sn-glycerol-3-phosphate acyltransferase gamma / LPAAT-g1)	Hs00987571_m1
AGPAT4	(1-acyl-sn-glycerol-3-phosphate acyltransferase / LPAAT-d)	Hs00220031_m1
AGPAT5	(1-acyl-sn-glycerol-3-phosphate acyltransferase / LPAAT-e)	Hs00218010_m1
AGPAT9	(1-acylglycerol-3-phosphate O-acyltransferase 9/ LPAAT-theta)	Hs00262010_m1
CDS1	(phosphatidate cytidyltransferase)	Hs00181633_m1
PCYT1A	(choline-phosphate cytidyltransferase)	Hs00192339_m1
PCYT2	(ethanolamine-phosphate cytidyltransferase)	Hs00161098_m1
PDE3B	(phosphodiesterase type 3)	Hs01057215_m1
FDFT1	(farnesyl-diphosphate farnesyltransferase 1)	Hs00926054_m1
SREBF1	(sterol regulatory element binding transcription factor 1)	Hs01088691_m1
BCL2	(B-cell CLL/lymphoma 2)	Hs99999018_m1
CD163	Macrophage and monocyte marker	Hs01016661_m1
CPT1A	(carnitine palmitoyltransferase 1A)	Hs00912676_m1

360

361 *Cytokines measurement in culture media*

362 Cytokines protein levels in culture media of 3T3-L1 CAR Δ 1 adipocytes and RAW

363 264.7 macrophages were measured by Luminex technology with a MILLIPLEX

364 Analyzer Luminex 200x Ponenet System (MCYTOMAG-70K-08 Mouse Cytokine

365 MAGNETIC Kit; Merck Millipore).

366

367

368 *Analysis of cellular redox status*

369 To detect ROS (superoxide) formation, MitoSOX Red (M36008 - Life Technologies)
370 fluorescence was measured by flow cytometry. RAW 264 cells were infected with 100
371 moi AdCPT1AM (or AdGFP as control) for 48h; then 16h prior to ROS measurement,
372 macrophages were treated with 0.75 mM palmitate BSA-conjugated (or with BSA as
373 control). Medium was removed and cells were incubated for 30 min with PBS
374 containing 5 μ M MitoSOX Red. The labeled macrophages were washed three times
375 with HBSS/Ca/Mg, pelleted, resuspended in 300 μ l HBSS/Ca/Mg and fixed by adding
376 1.2 ml absolute ethanol and keeping them at -20°C for 5 minutes. Cells were pelleted
377 again and resuspended in HBSS/Ca/Mg containing 3 μ M DAPI, to mark their nuclei.
378 Then macrophages were analyzed by flow cytometry (Gallios Cytometer - Beckman
379 Coulter). The fluorescence intensity of MitoSOX Red was measured using excitation at
380 510 nm and emission at 580 nm.

381

382 *Statistical analysis*

383 Data are expressed as the mean \pm SEM and analyzed statistically using Student's *t*-test
384 (column analysis) or two-way ANOVA (grouped analysis). All figures and statistical
385 analyses were generated using GraphPad Prism 6. $P < 0.05$ was considered statistically
386 significant. For human data statistical analyses were performed with SPSS 12.0 (SPSS).
387 Results are expressed as mean \pm SD. The non-normally distributed variables were
388 represented as the median (interquartile range). Categorical variables were reported by
389 number (percentages). Student's *t* test analysis was used to compare the mean value of
390 normally distributed continuous variables. Variables with a non-Gaussian distribution
391 were analyzed by using non-parametric test (Kruskal-Wallis, or Mann-Whitney test for

392 independent samples or Wilcoxon test for related samples when necessary).
393 Associations between continuous variables are sought by correlation analyses. Finally a
394 stepwise multiple linear regression analysis is performed to determine independent
395 variables associated with CPT1A gene expression levels in SAT and VAT depot.
396 Results are expressed as unstandardized coefficient (B), and 95% confidence interval
397 for B (95%CI(B)). Differences are considered significant if a computed two-tailed
398 probability value (P) is < 0.05 .
399
400

401 **RESULTS**

402 **CPT1A expression pattern in human adipose tissue from obese and diabetic** 403 **patients**

404 Visceral and subcutaneous adipose tissue (VAT and SAT, respectively) were
405 analyzed from both an obesity cohort (lean, overweight and obese patients) and a T2D
406 cohort (control and T2D patients). Tables 1 and 2 show the phenotypic and metabolic
407 characteristics and CPT1A expression levels of the subjects. No differences in CPT1A
408 gene expression levels either in SAT or in VAT depots were observed when comparing
409 with the non-obese or the non-diabetic counterparts (Fig. 1A and B; Tables 1 and 2).
410 However, in the obesity cohort, CPT1A mRNA expression was significantly higher in
411 lean and overweight VAT than in SAT (Fig. 1A). This difference was lost in the obese
412 patients. These results were corroborated by Western blot with human adipose tissue of
413 several lean and obese individuals (Fig. 1C and D, $P=0.015$). Similar results were
414 obtained in the T2D cohort, where control subjects showed significantly higher CPT1A
415 mRNA levels in VAT *vs.* SAT (Fig. 1B). However, this difference disappeared in T2D
416 patients. Despite T2D patients showed a trend to express higher CPT1A levels in SAT
417 and VAT compared to controls (on the opposite than in the obese subjects) this
418 difference was non-significant. Since CPT1B isoform is also expressed in human
419 adipose tissue we analyzed CPT1B mRNA (Fig. 1E and F) and protein (data not shown)
420 levels in human VAT and SAT of the obesity and the T2D cohort. No differences were
421 seen among the groups.

422 In order to establish the main relationship between CPT1A gene expression and
423 key adipocyte genes involved in differentiation and metabolic pathways we explored a
424 panel of genes (listed in Material and Methods) both in SAT and VAT depots of the
425 obesity cohort. Results are shown from those genes that changed the most (up or down)

426 (Tables 3 and 4). Simple association analysis showed an inverse correlation between
427 CPT1A and PPAR- γ in SAT ($r = -0.38$, $P = 0.002$) (Table 3). Positive CPT1A correlation
428 both in VAT and SAT was found with AGPAT5 (phospholipid biosynthesis), SREBF1
429 (glucose and lipid metabolism), BCL2 (anti-apoptosis) and CD163 (macrophage
430 marker) (Table 3).

431 To study the main determinants of CPT1A gene expression levels, a stepwise
432 multiple regression analysis was performed, including the above-mentioned bivariate
433 associations and confounding factors such as BMI, age and gender. This model showed
434 that SAT CPT1A was positively associated with AGPAT5, SREBF1 and CD163 and
435 that VAT CPT1A was positively correlated with SREBF1 and CD163 and negatively
436 with age and PPAR- γ (Table 4). The inverse relationship between CPT1A and PPAR- γ
437 was corroborated with the human adipocyte cell line SGBS. CPT1A mRNA expression
438 dropped to a new steady state in adipocytes that was 11% of its expression in fibroblasts
439 (data not shown).

440

441 **CPT1A is highly expressed in human adipose tissue macrophages**

442 To determine the cellular distribution of CPT1A gene and protein in human
443 adipose tissue biopsies, we performed qRT-PCR and immunostaining analysis on both
444 adipose and stromal-vascular fraction (SVF). CPT1A mRNA levels were 42.6-, and
445 43.4-fold increased in the SVF compared to mature adipocytes in both human SAT
446 ($P < 0.05$) and VAT ($P < 0.05$), respectively (Fig. 2A). Immunohistological examination
447 of SAT from obese subjects revealed CPT1A+ cells mostly in the SVF (Fig. 2B).
448 Immunofluorescence detection showed a bright staining pattern in cells resembling
449 adipose tissue macrophages. Co-staining analysis using CPT1A and CD68 (a
450 macrophage marker) antibodies confirmed the expression of CPT1A in macrophages

451 (Fig. 2C). Macrophages seem to localize forming the so-called “crown-like structures”
452 surrounding the adipocytes.

453

454 **CPT1AM-expressing adipocytes show enhanced FAO and reduced TG content**

455 To further study the role of CPT1A in adipocytes and macrophages we decided
456 to continue with *in vitro* studies. Since 3T3-L1 adipocytes are inefficiently infected with
457 adenovirus we decided to use the high-infection efficiency white adipocyte cell culture
458 line, 3T3-L1 CARΔ1 adipocytes (31) (Fig. 3A). Cells were transduced for the first time
459 with adenoviruses carrying the CPT1AM gene or GFP as a control. Interestingly,
460 CPT1AM-expressing adipocytes were partially protected from palmitate induced cell
461 death (Fig. 3C).

462 CPT1A mRNA, protein and activity levels were increased in CPT1AM-
463 expressing adipocytes compared to GFP control cells (Fig. 4A-C). CPT1AM-expressing
464 adipocytes retained most of the CPT1 activity after incubation with the CPT1A inhibitor
465 malonyl-CoA (Fig. 4C). FAO rate was concordantly enhanced (1.37-fold increase,
466 $P < 0.05$) in CPT1AM-expressing adipocytes (Fig. 4D). FA undergoing β -oxidation yield
467 acetyl-CoA moieties that have two main possible fates: (1) complete oxidation to CO_2
468 and ATP production, or (2) conversion to ketone bodies (mainly in the liver). Here, total
469 FAO rate was calculated as the sum of acid soluble products plus CO_2 oxidation.
470 CPT1AM expression blocked the palmitate-induced increase in TG content (Fig. 4E).

471

472 **Enhanced adipocyte FAO improves insulin sensitivity and reduces inflammation**

473 We examined the effect of increased FAO on insulin sensitivity and
474 inflammatory responses in 3T3-L1 CARΔ1 adipocytes infected with AdCPT1AM.
475 Palmitate-induced decrease in insulin-stimulated Akt phosphorylation and insulin

476 receptor beta (IRbeta) protein levels was partially restored in CPT1AM-expressing
477 adipocytes (Fig. 4F-H). Palmitate-induced increase of proinflammatory markers (IL-1 β ,
478 MCP-1 and IL-1 α) mRNA and protein levels was blunted in CPT1AM-expressing
479 adipocytes (Fig. 4I-K). Several palmitate concentrations and times of incubation were
480 used to better fit the different dose- and time-response of the cytokines and parameters
481 measured. Consistent with previous studies (9, 11), palmitate incubation raised
482 cytokines expression by 2-3-fold.

483

484 **Increased FAO in CPT1AM-expressing macrophages protects from palmitate-** 485 **induced TG accumulation**

486 Since CPT1A was highly expressed in the SVF, and particularly in
487 macrophages, of human adipose tissue we decided to further analyze the effect of an
488 increased FAO on cultured macrophages. RAW 264.7 macrophages were efficiently
489 infected with AdCPT1AM (Fig. 3B). CPT1AM-expressing macrophages were protected
490 from palmitate induced cell death (Fig. 3D). CPT1AM-expressing macrophages showed
491 a 2.4-fold (P<0.01) increase in CPT1A mRNA levels, 6.6-fold (P<0.01) increase in
492 protein levels and 2.2-fold (P<0.05) increase in activity levels (Fig. 5A-C). In addition,
493 we showed that malonyl-CoA did not inhibit CPT1 activity in CPT1AM-expressing
494 macrophages (Fig. 5C). CPT1AM-expressing macrophages showed a 1.5-fold increase
495 in FAO rate compared to GFP control cells (Fig. 5D, P<0.05) and a total restoration in
496 palmitate-induced enhancement of TG content (Fig. 5E and F).

497

498 **Enhanced macrophage FAO reduced inflammation, ER stress and ROS damage**

499 Palmitate-induced increase in proinflammatory cytokines (TNF- α , MCP-1, IL-
500 1 β , TLR-4 and IL-12p40) and ER stress markers (CHOP, GRP78, PDI and EDEM)

501 mRNA and protein levels was blunted in CPT1AM-expressing macrophages (Fig. 6A,
502 B, D and E)). Consistent with previous studies (18, 47, 48), palmitate incubation raised
503 cytokines expression by 2-3-fold. No differences were seen in anti-inflammatory
504 markers such as IL-10, Mgl-1 and IL-4 in CPT1AM-expressing cells incubated with or
505 without palmitate (Fig. 6C). Incubation with etomoxir, a permanent inhibitor of CPT1A,
506 counteracted the reduction of MCP-1 expression seen in CPT1AM-expressing cells
507 incubated with palmitate (data not shown). We also studied the effect of enhanced FAO
508 in RAW 264.7 macrophages on palmitate-induced ROS damage by protein carbonyl
509 content analysis. Palmitate-induced ROS damage was reduced in CPT1AM-expressing
510 macrophages (Fig. 6F). This reduction was not detected when ROS (superoxide) was
511 directly measured by using the MitoSOX Red probe (Fig. 6G).

512

513 **DISCUSSION**

514 The obesity epidemic has put a spotlight on the adipose tissue as a key player in
515 obesity-induced insulin resistance (38). Obese individuals and those with T2D have
516 lower FAO rates (17, 19, 37). Although these data were reported in skeletal muscle, we
517 expected to see reduced CPT1A expression levels in the adipose tissue of both obese
518 and T2D patients. However, no differences were seen in CPT1A mRNA expression
519 between the obese or T2D and their respective controls either in VAT or in SAT. Other
520 authors have reported a decrease in VAT CPT1 mRNA and protein levels in obese
521 individuals (20). However, the authors did not specify which of the CPT1 isoforms was
522 measured in VAT: CPT1A or CPT1B. We showed that CPT1A expression is higher in
523 adipose tissue macrophages than in mature adipocytes. Since the obese adipose tissue
524 has higher infiltration of immune cells such as macrophages, we postulate that the
525 putative decrement of CPT1A expression in obese individuals could be compensated by
526 increased expression from the infiltrated macrophages and thus, no differences are seen
527 between the groups. CPT1B isoform is also expressed in human adipose tissue and it
528 has been shown to raise FAO in metabolic tissues such as skeletal muscle (3). Thus, we
529 measured mRNA and protein levels in the obese and T2D cohorts. However, no
530 differences were seen among the groups indicating that CPT1B expression is not
531 changed by obesity and T2D.

532 We found that in insulin sensitive individuals (control and overweight patients
533 from the obese cohort and control patients from the T2D cohort) CPT1A mRNA
534 expression was higher in VAT than in SAT. However, no differences between VAT and
535 SAT were seen in the more insulin-resistant individuals with a more pro-inflammatory
536 environment: obese and T2D patients. A similar phenomenon was described for T
537 regulatory cells, described to have anti-inflammatory properties and to improve obesity-

538 induced insulin resistance (7). The authors reported that VAT and SAT of healthy
539 individuals had similar low numbers of T regulatory cells at birth, with a progressive
540 accumulation over time in the VAT, though not the SAT. Our results suggest a CPT1A
541 expression balance between SAT and VAT depots that may be disturbed in obese and
542 T2D patients. The difference in CPT1A expression between these two fat depots is
543 potentially crucial, given the association of VAT, but not SAT with insulin resistance
544 (1, 52). It might indicate, in healthy individuals, a potential protective role of CPT1A in
545 the more insulin-resistant associated VAT.

546 Gene expression analysis revealed a negative association between CPT1A and
547 the adipocyte marker of differentiation PPAR- γ . This is consistent with the fact that
548 while white adipocytes mature they shift their lipid preferences to storage rather than
549 oxidation. Aging was associated with reduced CPT1A expression in VAT. This might
550 reflect a potential protective role of CPT1A expression in VAT, which is lost with age.
551 Considering that VAT accretion is a hallmark of aging and especially, it is a stronger
552 risk factor for comorbidities and mortality (23), we speculate a favorable role of
553 enhanced CPT1A expression in age metabolic decline and related pathological
554 conditions. Positive correlation both in VAT and SAT CPT1A was found with
555 AGPAT5, SREBF1, BCL2 and CD163. These results may indicate a potential role of
556 CPT1A in lipid biosynthesis processes (AGPAT5), glucose and lipid metabolism
557 (SREBF1) and in protecting adipose tissue from apoptosis (BCL2). The positive
558 association between CPT1A and CD163 (macrophage marker) was not surprising given
559 the higher CPT1A expression in macrophages than in adipocytes (Fig. 2).

560 We are aware that many of the above mentioned associations may be secondary
561 to obesity or T2D and that no causal relationship may be inferred with this study design.
562 In order to prove the causality of some of these observations we performed *in vitro*

563 studies directly targeting adipocytes and macrophages to burn off the excess lipids
564 through an increase in FAO. We used the high-infection efficiency adipocyte cell line,
565 3T3-L1 CARΔ1 (31), to express for the first time CPT1AM through adenoviral
566 infection. Noteworthy, white adipocytes are designed to store lipids rather than to
567 oxidize them. Thus, CPT1 activity in WAT is lower than in other tissues (6). However,
568 CPT1AM-expressing adipocytes showed a 4.3-fold increase in CPT1 activity that was
569 not inhibited despite incubation with high concentrations of malonyl-CoA. Since
570 increased lipid accumulation, inflammation, ER stress and ROS-induced protein
571 damage trigger metabolic diseases we decided to measure TG content, inflammation,
572 ER stress and ROS damage as important mechanisms that could explain the potential
573 protective effect of CPT1AM expression. Enhanced FAO led to complete restoration of
574 TG content, improved insulin signaling (measured as pAkt), increased IRbeta
575 expression and cell viability and reduced inflammation in palmitate-incubated
576 CPT1AM-expressing adipocytes. CPT1AM-expressing adipocytes showed a general
577 improvement in lipid-induced derangements as a consequence of increased FA flux
578 through mitochondria. However, enhanced FA flux in the absence of a concomitant
579 dissipation of FAO metabolites has been associated with increased ROS damage (35)
580 and inflammation (8, 21, 43). Interestingly, while no differences were seen in ER or
581 oxidative stress (data not shown), CPT1AM-expressing adipocytes showed a significant
582 decrease in proinflammatory mediators such as IL-1 β and MCP-1. The favorable role of
583 CPT1A in adipocytes to attenuate FA evoked insulin resistance and inflammation has
584 been also described to act via suppression of JNK (9). These results suggest that factors
585 other than a FAO increase *per se* are responsible for ROS production and inflammation.
586 Accumulation of toxic substances (diacylglycerol or ceramides) (49), hypoxia (15), as
587 well as cytokines (42) might participate in the induction of ROS damage and the

588 inflammatory state. Several researchers have demonstrated that enhanced FAO through
589 CPT1A or CPT1AM expression results in a decrease in relevant lipid mediators
590 involved in inflammation and insulin resistance such as diacylglycerol, intracellular
591 NEFAs (non-esterified FA), free FA, ceramides and TG (3, 9, 13, 26, 29, 40, 45). While
592 some authors (3) didn't see changes in skeletal muscle acylcarnitines' profile our group
593 has shown an increase in several acylcarnitines in CPT1AM-expressing neurons (25).

594 FA undergoing β -oxidation yield acetyl-CoA moieties that have two main
595 possible fates: (1) entry to the Krebs cycle for complete oxidation and ATP production,
596 or (2) conversion to ketone bodies (mainly in the liver). We observed increased FAO to
597 CO₂ and acid soluble products in CPT1AM-expressing adipocytes and macrophages.
598 CPT1AM expression in liver has been shown to enhance ATP and ketone bodies
599 production with no changes in glucose oxidation (29), (13). Altogether, this indicates a
600 metabolic rate switch towards FA.

601 Monocytes were the first immune cells reported to infiltrate obese adipose
602 tissue, differentiate to macrophages, produce inflammatory cytokines and trigger insulin
603 resistance (56, 57). Thus, we examined whether CPT1AM expression could play a
604 protective role in obesity-induced macrophage derangements. We found that, in human
605 WAT, CPT1A is highly expressed in SVF compared to adipocytes. This happened both
606 in human VAT and SAT. A closer histological and immunofluorescence examination
607 showed that macrophages present in the adipose tissue expressed CPT1A. This does not
608 rule out CPT1A expression in other immune cells also present in the adipose tissue such
609 as T and B cells, T regulatory cells, and mast cells.

610 Given the high CPT1A expression in human adipose tissue macrophages, we
611 decided to study the effect of CPT1AM in RAW 264.7 macrophages. A permanently
612 enhanced FAO rate in CPT1AM-expressing macrophages led to a complete restoration

613 of palmitate-induced increase in TG content, and a decrease in inflammation, ER and
614 oxidative stress without affecting cell viability. Recent data show that FAO is capable
615 of regulating the degree of acyl chain saturation in ER phospholipids (28). Since
616 increasing the degree of saturation in ER phospholipids has been described to directly
617 activate ER stress and inflammation (28) this might provide a mechanistic link to how
618 FAO alleviates ER stress under palmitate loading. Thus, enhancing CPT1A expression
619 in macrophages may be a potential approach to fight against obesity-induced disorders.

620 In conclusion, we have shown that CPT1A expression was higher in human
621 adipose tissue macrophages than in mature adipocytes and that it was differentially
622 expressed in VAT vs. SAT. Further *in vitro* studies demonstrated that an increase in
623 FAO in lipid-treated adipocytes and macrophages reduced TG content and
624 inflammatory levels, improved insulin sensitivity in adipocytes, and reduced ER stress
625 and ROS damage in macrophages. Adipocyte specific knockout or transgenic animal
626 models for CPT1A would be especially relevant to elucidate its potential protection
627 against obesity-induced insulin resistance *in vivo*. Our data support the hypothesis that
628 pharmacological or genetic strategies to enhance FAO may be beneficial for the
629 treatment of chronic inflammatory pathologies such as obesity and T2D.

630

631 **Funding**

632 This study was supported by the Spanish Ministry of Science and Innovation (Grants
633 SAF2010-20039 and SAF2013-45887-R to LH, SAF2011-30520-C02-01 to DS,
634 PI11/00085 to JJV, SAF2012-33014 to BP, SAF2012-36186 to SF-V, SAF2012-30708
635 to MVC, SAF2011-23626 to FV and doctoral fellowships to MIM and JFM), by the
636 CIBER Fisiopatología de la Obesidad y la Nutrición (CIBERObn) (Grant CB06/03/0001
637 to DS) and CIBER Diabetes y Enfermedades Metabólicas Asociadas (CIBERDEM)
638 (Grant CB07/08/0003 to MVC), Instituto de Salud Carlos III, by the European Union
639 (BetaBat project FP7-277713 to FV), by the European Foundation for the Study of
640 Diabetes (EFSD)/Lilly and EFSD/Janssen-Rising Star research fellowships to LH and
641 by the L'Oréal-UNESCO “For Women in Science” research fellowship to LH. MW is a
642 recipient of the Ciência sem Fronteiras-CNPq fellowship (237976/2012-9).

643

644 **Acknowledgements**

645 We thank Professor F.G. Hegardt and Dr. G. Asins for helpful comments and
646 suggestions, A. Orozco for technical assistance and R. Rycroft from the Language
647 Service of the University of Barcelona for valuable assistance in the preparation of the
648 English manuscript. We also thank D. Orlicky for kindly providing 3T3-L1 CARΔ1
649 adipocytes. SF-V acknowledges support from the “Miguel Servet” tenure track program
650 (CP10/00438) from the Fondo de Investigación Sanitaria (FIS) and co-financed by the
651 European Regional Development Fund (ERDF).

652

653 **Contribution statement**

654 All the authors contributed to the conception and design of the study. MIM, RF,
655 MW, MCD, JFM, LV, XE, MG-S, BP and LS carried out the experiments. All authors

656 contributed to the analysis and interpretation of data and revising it critically for
657 important intellectual content. MIM, RF, MCD, JFM, BP, JJV and LH wrote the
658 manuscript. All authors revised and approved the final manuscript.

659

660

661

662

663 REFERENCES

- 664 1. **Bosello O, Zamboni M.** Visceral obesity and metabolic syndrome. *Obes Rev* 1:
665 47–56, 2000.
- 666 2. **Brown NF, Hill JK, Esser V, Kirkland JL, Corkey BE, Foster DW, Garry
667 JDMC.** Mouse white adipocytes and 3T3-L1 cells display an anomalous pattern
668 of carnitine palmitoyltransferase (CPT) I isoform expression during
669 differentiation. *Biochem J* 231: 225–231, 1997.
- 670 3. **Bruce CR, Hoy AJ, Turner N, Watt MJ, Allen TL, Carpenter K, Cooney
671 GJ, Febbraio M a, Kraegen EW.** Overexpression of carnitine
672 palmitoyltransferase-1 in skeletal muscle is sufficient to enhance fatty acid
673 oxidation and improve high-fat diet-induced insulin resistance. *Diabetes* 58: 550–
674 8, 2009.
- 675 4. **Bruce CR, Hoy AJ, Turner N, Watt MJ, Allen TL, Carpenter K, Cooney
676 GJ, Febbraio MA, Kraegen EW.** Overexpression of carnitine
677 palmitoyltransferase-1 in skeletal muscle is sufficient to enhance fatty acid
678 oxidation and improve high-fat diet-induced insulin resistance. *Diabetes* 58: 550–
679 8, 2009.
- 680 5. **Davies LC, Jenkins SJ, Allen JE, Taylor PR.** Tissue-resident macrophages.
681 *Nat Immunol* 14: 986–95, 2013.
- 682 6. **Doh K-O, Kim Y-W, Park S-Y, Lee S-K, Park JS, Kim J-Y.** Interrelation
683 between long-chain fatty acid oxidation rate and carnitine palmitoyltransferase 1
684 activity with different isoforms in rat tissues. *Life Sci* 77: 435–43, 2005.
- 685 7. **Feuerer M, Herrero L, Cipolletta D, Naaz A, Wong J, Nayer A, Lee J,
686 Goldfine AB, Benoist C, Shoelson S, Mathis D.** Lean, but not obese, fat is
687 enriched for a unique population of regulatory T cells that affect metabolic
688 parameters. *Nat Med* 15: 930–939, 2009.
- 689 8. **Furukawa S, Fujita T, Shimabukuro M, Iwaki M, Yamada Y, Nakajima Y,
690 Nakayama O, Makishima M, Matsuda M, Shimomura I.** Increased oxidative
691 stress in obesity and its impact on metabolic syndrome. *J Clin Invest* 114: 1752–
692 1761, 2004.
- 693 9. **Gao X, Li K, Hui X, Kong X, Sweeney G, Wang Y, Xu A, Teng M, Liu P,
694 Wu D.** Carnitine palmitoyltransferase 1A prevents fatty acid-induced adipocyte
695 dysfunction through suppression of c-Jun N-terminal kinase. *Biochem J* 435:
696 723–732, 2011.
- 697 10. **Gesta S, Bezy O, Mori MA, Macotela Y, Lee KY, Kahn CR.** Mesodermal
698 developmental gene Tbx15 impairs adipocyte differentiation and mitochondrial
699 respiration. *Proc Natl Acad Sci U S A* 108: 2771–6, 2011.

- 700 11. **Hamada Y, Nagasaki H, Fujiya A, Seino Y, Shang Q-L, Suzuki T,**
701 **Hashimoto H, Oiso Y.** Involvement of de novo ceramide synthesis in pro-
702 inflammatory adipokine secretion and adipocyte-macrophage interaction. *J Nutr*
703 *Biochem* 25: 1309–16, 2014.
- 704 12. **Haslam DW, James WPT.** Obesity. *Lancet* 366: 1197–1209, 2005.
- 705 13. **Herrero L, Rubí B, Sebastián D, Serra D, Asins G, Maechler P, Prentki M,**
706 **Hegardt FG.** Alteration of the malonyl-CoA/carnitine palmitoyltransferase I
707 interaction in the beta-cell impairs glucose-induced insulin secretion. *Diabetes*
708 54: 462–471, 2005.
- 709 14. **Herrero L, Shapiro H, Nayer A, Lee J, Shoelson SE.** Inflammation and
710 adipose tissue macrophages in lipodystrophic mice. *Proc Natl Acad Sci U S A*
711 107: 240–245, 2010.
- 712 15. **Hosogai N, Fukuhara A, Oshima K, Miyata Y, Tanaka S, Segawa K,**
713 **Furukawa S, Tochino Y, Komuro R, Matsuda M, Shimomura I.** Adipose
714 tissue hypoxia in obesity and its impact on adipocytokine dysregulation. *Diabetes*
715 56: 901–911, 2007.
- 716 16. **Hotamisligil GS.** Endoplasmic reticulum stress and the inflammatory basis of
717 metabolic disease. *Cell* 140: 900–17, 2010.
- 718 17. **Houmard JA.** Intramuscular lipid oxidation and obesity. *Am J Physiol Regul*
719 *Integr Comp Physiol* 294: R1111–1116, 2008.
- 720 18. **Huang S, Rutkowski JM, Snodgrass RG, Ono-Moore KD, Schneider DA,**
721 **Newman JW, Adams SH, Hwang DH.** Saturated fatty acids activate TLR-
722 mediated proinflammatory signaling pathways. *J Lipid Res* 53: 2002–13, 2012.
- 723 19. **Kelley DE, He J, Menshikova E V, Ritov VB.** Dysfunction of Mitochondria in
724 Human Skeletal Muscle in Type 2 Diabetes. *Diabetes* 51: 2944–2950, 2002.
- 725 20. **Krishnan J, Danzer C, Simka T, Ukropec J, Walter KM, Kumpf S,**
726 **Mirtschink P, Ukropcova B, Gasperikova D, Pedrazzini T, Krek W.** Dietary
727 obesity-associated Hif1 α activation in adipocytes restricts fatty acid oxidation
728 and energy expenditure via suppression of the Sirt2-NAD⁺ system. *Genes Dev*
729 26: 259–70, 2012.
- 730 21. **Lin Y, Berg AH, Iyengar P, Lam TK, Giacca A, Combs TP, Rajala MW, Du**
731 **X, Rollman B, Li W, Hawkins M, Barzilai N, Rhodes CJ, Fantus IG,**
732 **Brownlee M, Scherer PE.** The hyperglycemia-induced inflammatory response
733 in adipocytes: the role of reactive oxygen species. *J Biol Chem* 280: 4617–4626,
734 2005.
- 735 22. **Mathis D.** Immunological goings-on in visceral adipose tissue. *Cell Metab* 17:
736 851–9, 2013.

- 737 23. **Matsuzawa Y, Shimomura I, Nakamura T, Keno Y, Tokunaga K.**
738 Pathophysiology and pathogenesis of visceral fat obesity. *Ann N Y Acad Sci* 748:
739 399–406, 1995.
- 740 24. **Matthews DR, Hosker JP, Rudenski AS, Naylor BA, Treacher DF, Turner**
741 **RC.** Homeostasis model assessment: insulin resistance and beta-cell function
742 from fasting plasma glucose and insulin concentrations in man. *Diabetologia* 28:
743 412–419, 1985.
- 744 25. **Mera P, Mir JF, Fabriàs G, Casas J, Costa ASH, Malandrino MI,**
745 **Fernández-López J-A, Remesar X, Gao S, Chohnan S, Rodríguez-Peña MS,**
746 **Petry H, Asins G, Hegardt FG, Herrero L, Serra D.** Long-term increased
747 carnitine palmitoyltransferase 1A expression in ventromedial hypothalamus causes
748 hyperphagia and alters the hypothalamic lipidomic profile. *PLoS One* 9: e97195,
749 2014.
- 750 26. **Monsénégo J, Mansouri A, Akkaoui M, Lenoir V, Esnous C, Fauveau V,**
751 **Tavernier V, Girard J, Prip-Buus C.** Enhancing liver mitochondrial fatty acid
752 oxidation capacity in obese mice improves insulin sensitivity independently of
753 hepatic steatosis. *J Hepatol* 56: 632–639, 2012.
- 754 27. **Morillas M, Gómez-Puertas P, Bentebibel A, Sellés E, Casals N, Valencia A,**
755 **Hegardt FG, Asins G, Serra D.** Identification of conserved amino acid residues
756 in rat liver carnitine palmitoyltransferase I critical for malonyl-CoA inhibition.
757 Mutation of methionine 593 abolishes malonyl-CoA inhibition. *J Biol Chem* 278:
758 9058–63, 2003.
- 759 28. **Namgaladze D, Lips S, Leiker TJ, Murphy RC, Ekroos K, Ferreiros N,**
760 **Geisslinger G, Brüne B.** Inhibition of macrophage fatty acid β -oxidation
761 exacerbates palmitate-induced inflammatory and endoplasmic reticulum stress
762 responses. *Diabetologia* 57: 1067–1077, 2014.
- 763 29. **Orellana-Gavalda JM, Herrero L, Malandrino MI, Paneda A, Sol**
764 **Rodríguez-Pena M, Petry H, Asins G, Van Deventer S, Hegardt FG, Serra**
765 **D.** Molecular therapy for obesity and diabetes based on a long-term increase in
766 hepatic fatty-acid oxidation. *Hepatology* 53: 821–832, 2011.
- 767 30. **Orellana-Gavaldà JM, Herrero L, Malandrino MI, Pañeda A, Sol**
768 **Rodríguez-Peña M, Petry H, Asins G, Van Deventer S, Hegardt FG, Serra**
769 **D.** Molecular therapy for obesity and diabetes based on a long-term increase in
770 hepatic fatty-acid oxidation. *Hepatology* 53: 821–832, 2011.
- 771 31. **Orlicky DJ, DeGregori J, Schaack J.** Construction of stable coxsackievirus and
772 adenovirus receptor-expressing 3T3-L1 cells. *J Lipid Res* 42: 910–915, 2001.
- 773 32. **Patti M-E, Corvera S.** The role of mitochondria in the pathogenesis of type 2
774 diabetes. *Endocr Rev* 31: 364–95, 2010.
- 775 33. **Perdomo G, Commerford SR, Richard A-MT, Adams SH, Corkey BE,**
776 **O’Doherty RM, Brown NF.** Increased beta-oxidation in muscle cells enhances

- 777 insulin-stimulated glucose metabolism and protects against fatty acid-induced
778 insulin resistance despite intramyocellular lipid accumulation. *J Biol Chem* 279:
779 27177–27186, 2004.
- 780 34. **Pérez-Pérez R, García-Santos E, Ortega-Delgado FJ, López JA, Camafeita**
781 **E, Ricart W, Fernández-Real J-M, Peral B.** Attenuated metabolism is a
782 hallmark of obesity as revealed by comparative proteomic analysis of human
783 omental adipose tissue. *J Proteomics* 75: 783–95, 2012.
- 784 35. **Pessayre D, Fromenty B, Mansouri A.** Mitochondrial injury in steatohepatitis.
785 *Eur J Gastroenterol Hepatol* 16: 1095–1105, 2004.
- 786 36. **Price N, van der Leij F, Jackson V, Corstorphine C, Thomson R, Sorensen**
787 **A, Zammit V.** A novel brain-expressed protein related to carnitine
788 palmitoyltransferase I. *Genomics* 80: 433–442, 2002.
- 789 37. **Ritov VB, Menshikova E V, He J, Ferrell RE, Goodpaster BH, Kelley DE.**
790 Deficiency of Subsarcolemmal Mitochondria in Obesity and Type 2 Diabetes.
791 *Diabetes* 54: 8–14, 2004.
- 792 38. **Rosen ED, Spiegelman BM.** What We Talk About When We Talk About Fat.
793 *Cell* 156: 20–44, 2014.
- 794 39. **Samuel VT, Shulman GI.** Mechanisms for insulin resistance: common threads
795 and missing links. *Cell* 148: 852–71, 2012.
- 796 40. **Sebastian D, Herrero L, Serra D, Asins G, Hegardt FG.** CPT I overexpression
797 protects L6E9 muscle cells from fatty acid-induced insulin resistance. *Am J*
798 *Physiol Endocrinol Metab* 292: E677–86, 2007.
- 799 41. **Sebastián D, Herrero L, Serra D, Asins G, Hegardt FG.** CPT I overexpression
800 protects L6E9 muscle cells from fatty acid-induced insulin resistance. *Am J*
801 *Physiol Endocrinol Metab* 292: E677–86, 2007.
- 802 42. **Shoelson SE, Herrero L, Naaz A.** Obesity, inflammation, and insulin resistance.
803 *Gastroenterology* 132: 2169–80, 2007.
- 804 43. **Shoelson SE, Lee J, Goldfine AB.** Inflammation and insulin resistance. *J Clin*
805 *Invest* 116: 1793–1801, 2006.
- 806 44. **Simoneau JA, Veerkamp JH, Turcotte LP, Kelley DE.** Markers of capacity to
807 utilize fatty acids in human skeletal muscle: relation to insulin resistance and
808 obesity and effects of weight loss. *FASEB J* 13: 2051–60, 1999.
- 809 45. **Stefanovic-Racic M, Perdomo G, Mantell BS, Sipula IJ, Brown NF,**
810 **O’Doherty RM.** A moderate increase in carnitine palmitoyltransferase 1a
811 activity is sufficient to substantially reduce hepatic triglyceride levels. *Am J*
812 *Physiol Endocrinol Metab* 294: E969–77, 2008.

- 813 46. **Stefanovic-Racic M, Perdomo G, Mantell BS, Sipula IJ, Brown NF,**
814 **O’Doherty RM.** A moderate increase in carnitine palmitoyltransferase 1a
815 activity is sufficient to substantially reduce hepatic triglyceride levels. *Am J*
816 *Physiol Endocrinol Metab* 294: E969–977, 2008.
- 817 47. **Suganami T, Nishida J, Ogawa Y.** A paracrine loop between adipocytes and
818 macrophages aggravates inflammatory changes: role of free fatty acids and tumor
819 necrosis factor alpha. *Arterioscler Thromb Vasc Biol* 25: 2062–8, 2005.
- 820 48. **Suganami T, Tanimoto-Koyama K, Nishida J, Itoh M, Yuan X, Mizuarai S,**
821 **Kotani H, Yamaoka S, Miyake K, Aoe S, Kamei Y, Ogawa Y.** Role of the
822 Toll-like receptor 4/NF-kappaB pathway in saturated fatty acid-induced
823 inflammatory changes in the interaction between adipocytes and macrophages.
824 *Arterioscler Thromb Vasc Biol* 27: 84–91, 2007.
- 825 49. **Summers SA.** Ceramides in insulin resistance and lipotoxicity. *Prog Lipid Res*
826 45: 42–72, 2006.
- 827 50. **Sun K, Kusminski CM, Scherer PE.** Review series Adipose tissue remodeling
828 and obesity. 121, 2011.
- 829 51. **Sun K, Wernstedt Asterholm I, Kusminski CM, Bueno AC, Wang Z V,**
830 **Pollard JW, Brekken R a, Scherer PE.** Dichotomous effects of VEGF-A on
831 adipose tissue dysfunction. *Proc Natl Acad Sci U S A* 109: 5874–5879, 2012.
- 832 52. **Tran TT, Yamamoto Y, Gesta S, Kahn CR.** Beneficial effects of subcutaneous
833 fat transplantation on metabolism. *Cell Metab* 7: 410–420, 2008.
- 834 53. **Villarroya F, Domingo P, Giralt M.** Lipodystrophy in HIV 1-infected patients:
835 lessons for obesity research. *Int J Obes (Lond)* 31: 1763–76, 2007.
- 836 54. **Virtue S, Vidal-Puig A.** Adipose tissue expandability, lipotoxicity and the
837 Metabolic Syndrome--an allostatic perspective. *Biochim Biophys Acta* 1801:
838 338–49, 2010.
- 839 55. **Wabitsch M, Brenner RE, Melzner I, Braun M, Moller P, Heinze E, Debatin**
840 **KM, Hauner H.** Characterization of a human preadipocyte cell strain with high
841 capacity for adipose differentiation. *Int J Obes Relat Metab Disord* 25: 8–15,
842 2001.
- 843 56. **Weisberg SP, McCann D, Desai M, Rosenbaum M, Leibel RL, Ferrante**
844 **AW.** Obesity is associated with macrophage accumulation in adipose tissue. *J*
845 *Clin Invest* 112: 1796–1808, 2003.
- 846 57. **Xu H, Barnes GT, Yang Q, Tan G, Yang D, Chou CJ, Sole J, Nichols A,**
847 **Ross JS, Tartaglia LA, Chen H.** Chronic inflammation in fat plays a crucial
848 role in the development of obesity-related insulin resistance. *J Clin Invest* 112:
849 1821–1830, 2003.

850

851 **Tables**

852 **Table 1.** Clinical, analytical and CPT1A gene expression analysis of the obesity cohort.

853 BMI: Body mass index; sIL-6: soluble Interleukine-6; SBP: systolic blood pressure;

854 DBP: Diastolic blood pressure. Values are expressed as mean \pm SD or median

855 (interquartile range) for a non-Gaussian distributed variables. Differences *vs.* Lean:

856 *P<0.001; ¶P<0.05. Differences *vs.* Overweight: #P<0.001; §P<0.05. †P<0.05 SAT *vs.*

857 VAT expression.

858

859 **Table 2.** Clinical, analytical and CPT1A gene expression analysis of the T2D cohort.

860 BMI: Body mass index; sIL-6: soluble Interleukine-6; SBP: systolic blood pressure;

861 DBP: Diastolic blood pressure. Values are expressed as mean \pm SD or median

862 (interquartile range) for a non-Gaussian distributed variables. Differences *vs.* controls:

863 *P<0.001; ¶P<0.05. Differences between SAT and VAT in the same group: †P=0.03.

864

865 **Table 3.** Bivariate correlation analysis of CPT1A gene expression levels with several

866 genes in human VAT and SAT of the obesity cohort. PPAR- γ , Peroxisome proliferator-

867 activated receptor gamma; AGPAT5, 1-acylglycerol-3-phosphate O-acyltransferase 5;

868 SREBF1, sterol regulatory element binding transcription factor 1; BCL2, B-cell

869 CLL/lymphoma 2; CD163, macrophage and monocyte marker; p<0.005 for all

870 correlations.

871

872 **Table 4.** Multiple regression analysis for CPT1A in VAT and SAT as dependent

873 variable in the obesity cohort. Independent variables included in the model: age, gender,

874 body mass index (BMI), peroxisome proliferator-activated receptor alpha (PPAR- α),

875 peroxisome proliferator-activated receptor gamma (PPAR- γ), 1-acylglycerol-3-

876 phosphate O-acyltransferase 5 (AGPAT5), sterol regulatory element binding
877 transcription factor 1 (SREBF1), B-cell CLL/lymphoma 2 (BCL2) and macrophage and
878 monocyte marker (CD163) gene expression levels. β st: standardized beta coefficient.
879 CI: Confidence Interval.
880

881 **Figure legends**

882 **Fig. 1.** CPT1 gene and protein expression in human adipose tissue. **(A, B)** CPT1A
883 relative mRNA levels in human VAT and SAT of the obesity (A) or the T2D (B)
884 cohort. Number of individuals: 19 lean, 28 overweight, 15 obese, 36 control and 11
885 T2D (See Table 1 and 2 for more details). **(C, D)** CPT1A protein levels in human VAT
886 and SAT of seven lean individuals (P1-P7) (C) and three obese individuals (D). **(E, F)**
887 CPT1B relative mRNA levels in human VAT and SAT of the obesity (E) or the T2D
888 (F) cohort. *P<0.05.

889

890 **Fig. 2.** CPT1A is highly expressed in human adipose tissue macrophages. **(A)** CPT1A
891 mRNA levels in both adipose (AD) and stromal-vascular fraction (SVF) of human VAT
892 and SAT. n=4. *P<0.05. **(B)** Immunohistochemical detection of CPT1A (brown) in
893 SAT of obese subjects. **(C)** Immunofluorescence staining of CPT1A (red) and CD68
894 (green) proteins in SAT of obese individuals. The counterstaining of nuclei (DAPI) is
895 shown in blue. Images are representative of adipose tissue preparations collected from
896 three subjects.

897

898 **Fig. 3.** Adenovirus infection efficiency and viability in 3T3-L1 CARΔ1 adipocytes and
899 RAW 264.7 macrophages. Images were taken from **(A)** AdGFP-infected 3T3-L1
900 CARΔ1 adipocytes (50% infection) or **(B)** RAW 264.7 macrophages (70% infection)
901 48h or 72h after the infection, respectively. **(C, D)** Cell viability of (C) 3T3-L1 CARΔ1
902 adipocytes or (D) RAW 264.7 macrophages infected with AdGFP or AdCPT1AM and
903 incubated for 24h with 1mM or 0.3mM palmitate (PA), respectively.

904

905 **Fig. 4** Enhanced FAO in 3T3-L1 CARΔ1 adipocytes improves lipid-induced TG
906 accumulation, insulin sensitivity and inflammation. Relative CPT1A mRNA expression
907 (A) and protein levels (B) in AdGFP- or AdCPT1AM-infected 3T3-L1 CARΔ1
908 adipocytes. (C) CPT1 activity from mitochondria-enriched cell fractions incubated (or
909 not) with 100 μM malonyl-CoA. (D) Total FAO rate represented as the sum of acid
910 soluble products plus CO₂ oxidation. (E) TG content of adipocytes treated for 24 h with
911 1mM palmitate (PA). (F) Insulin signaling in GFP- and CPT1AM-expressing
912 adipocytes incubated with 0.3mM PA for 24 h as indicated by Western blotting of
913 insulin-induced Akt phosphorylation (pAkt) and IRbeta. (G) Quantification of pAkt
914 normalized by total Akt (fold change of arbitrary units, A.U.). (H) Quantification of
915 IRbeta normalized by β-actin. (I, J) Relative mRNA expression from GFP- or CPT1A-
916 expressing adipocytes incubated with 1mM PA for 24 h. (K) Protein levels of IL-1α in
917 the culture media of GFP- or CPT1A-expressing adipocytes incubated with 1mM PA
918 for 6 h. Shown representative experiments out of 3. n=3-6. *P<0.05.

919

920 **Fig. 5.** Enhanced FAO and reduced TG content in CPT1AM-expressing RAW 264.7
921 macrophages. Relative CPT1A mRNA expression (A) and protein levels (B) in AdGFP-
922 or AdCPT1AM-infected macrophages. (C) CPT1 activity from mitochondria-enriched
923 cell fractions incubated (or not) with 100 μM malonyl-CoA. (D) Total FAO rate
924 measured as the sum of acid soluble products plus CO₂ oxidation. (E) TG content and
925 (F) Oil Red O staining of macrophages treated for 18 h with 0.75 mM palmitate (PA).
926 Shown representative experiments out of 3. n=3-6. *P<0.05.

927

928 **Fig. 6.** CPT1AM expression reduced inflammation, ER stress and ROS damage in
929 RAW 264.7 macrophages. (A, C, D) Relative mRNA gene expression from

930 macrophages incubated with 0.5 mM palmitate (PA) for 8 h (TNF- α and MCP-1) or 0.3
931 mM PA for 24 h (IL-10, Mgl-1, IL-4, IL-1 β , TLR-4, CHOP, GRP78, PDI and EDEM).
932 **(B)** Protein levels of IL-12p40 in the culture media of macrophages incubated with 0.3
933 mM PA for 24 h. **(E)** CHOP protein levels and quantification in macrophages incubated
934 with 0.5 mM PA for 8 h **(F)** Protein carbonyl content analysis and quantification in
935 macrophages incubated with 0.75 mM PA for 18 h. **(G)** Measurement of ROS
936 (superoxide) using the MitoSOX Red probe. Shown representative experiments out of
937 3. n=3-4 *P<0.05.
938

Table 1

	Lean BMI<25 (13 male; 6 female)	Overweight 25=<BMI<30 (16 male; 12 female)	Obese BMI>=30 (9 male; 6 female)
Age (years)	51.7 ± 16.0	57.1 ± 15.0	57.4 ± 12.8
BMI (kg/m ²)	23.6 (22.1-24.2)	27.2 (26.5-27.9)*	32.1 (30.8-33.6)*#
Waist (cm)	83.0 (79.0-90.0)	97.0 (90.5-100.0)*	107.0 (100.0-117.2)*#
Cholesterol (mM)	5.2 ± 1.2	4.9 ± 1.0	5.2 ± 0.8
HDL-chol (mM)	1.5 ± 0.5	1.3 ± 0.3	1.4 ± 0.3
Triglycerides (mM)	1.0 (0.7-1.6)	1.1 (0.8-1.5)	1.0 (0.7-1.3)
Glucose (mM)	4.8 ± 0.7	5.5 ± 0.5*	5.6 ± 0.5*
Insulin (μIU/ml)	3.4 (2.1-6.7)	4.0 (2.8-7.2)	6.6 (4.5-16.5)¶
HOMA-IR	0.75 (0.54-1.83)	1.01 (0.52-2.09)	1.60 (1.19-4.79)¶
sIL-6 (pg/ml)	1.4 (1.1-2.5)	1.0 (0.7-2.2)	2.5 (1.4-5.2) §
SBP (mmHg)	120 (120-127)	130 (121-140)	145 (130-160)*§
DBP (mmHg)	70 (60-80)	70 (70-80)	80 (78-90)¶
SAT <i>CPT1A</i>	0.85 (0.66-1.14)†	1.15 (0.85-1.60)†	0.86 (0.72-1.81)
VAT <i>CPT1A</i>	1.31 (1.07-2.50)	1.42 (0.97-3.00)	1.07 (0.84-1.76)

Table 2

	Control (21 male, 15 female)	Type2 Diabetes (5 male, 6 female)
Age (years)	61.6 ± 10.6	66.1 ± 8.6
BMI (kg/m ²)	28.6 (27.0-31.5)	28.7 (26.9-30.4)
Waist (cm)	100.0 (94.0-107.0)	97.0 (94.0-102.0)
Cholesterol (mM)	5.1 ± 0.9	4.7 ± 1.2
HDL-chol (mM)	1.4 (1.2-1.6)	1.2 (1.0-1.9)
Triglycerides (mM)	1.0 (0.7-1.5)	1.7 (1.2-2.3)¶
NEFA (µM)	775.5 ± 275.1	926.4 ± 412.3
Glycerol (µM)	135.2 (117.2-222.3)	301.6 (209.6-465.3)¶
Glucose (mM)	5.6 (5.3-5.8)	8.3 (7.0-10.1)*
Insulin (µIU/ml)	4.5 (3.5-7.7)	10.2 (3.5-21.4)
HOMA-IR	1.22 (0.89-2.10)	3.66 (1.71-23.66)¶
sIL-6 (pg/ml)	1.4 (1.0-2.6)	1.5 (1.0-2.4)
SBP (mmHg)	140 (130-150)	140 (124-156)
DBP (mmHg)	80 (70-80)	80(63-83)
SAT <i>CPT1A</i>	1.08 (0.79-1.59)†	1.70 (1.03-2.18)
VAT <i>CPT1A</i>	1.39 (0.87-2.28)	1.57 (0.98-1.96)

Table 3

	CPT1A	
	SAT	VAT
	R	R
<i>PPAR-γ</i>	-0.382	
<i>AGPAT5</i>	0.639	0.714
<i>SREBF1</i>	0.525	0.757
<i>BCL2</i>	0.639	0.580
<i>CD163</i>	0.731	0.716

Table 4SAT (R^2 of the model: 0.71)

Independent variables	B (95% CI)	β st	<i>p</i>
CD163	0.34 (0.20 – 0.49)	0.446	<0.0001
AGPAT5	0.64 (0.33 – 0.95)	0.345	<0.0001
SREBF1	0.19 (0.06 – 0.33)	0.245	0.006

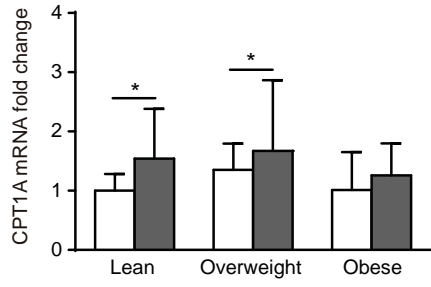
VAT (R^2 of the model: 0.70)

Independent variables	B (95% CI)	β st	<i>p</i>
CD163	0.34 (0.21 – 0.48)	0.569	<0.0001
Age	-0.15 (-0.025 – -0.004)	-0.22	0.006
SREBF1	0.413 (0.13 – 0.69)	0.323	0.005
PPAR- γ	-0.29 (-0.53 – -0.05)	-0.19	0.017

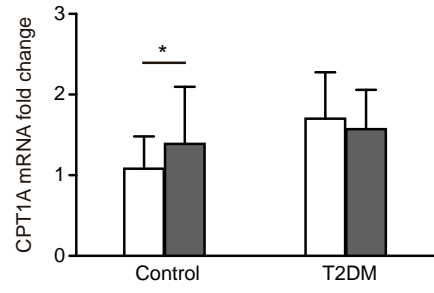
Figure 1

□ SAT ■ VAT

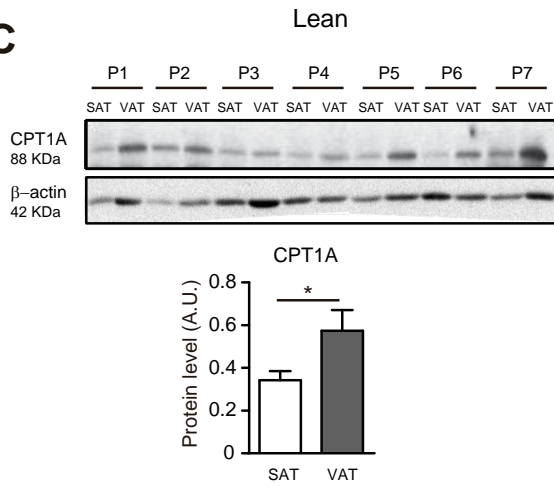
A



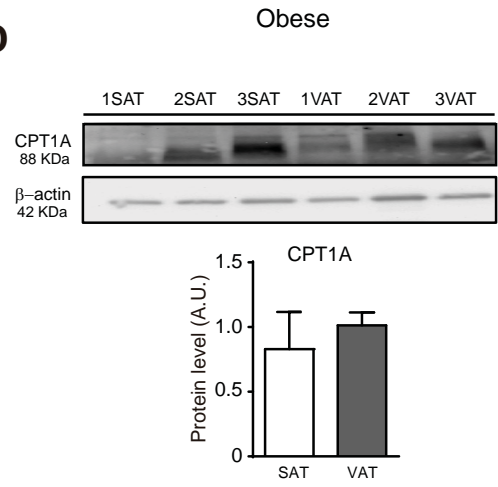
B



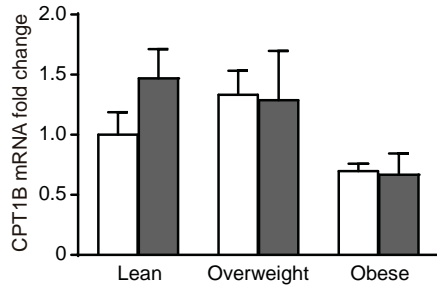
C



D



E



F

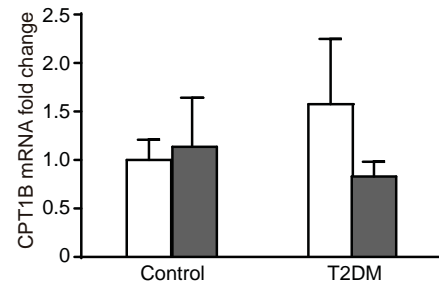


Figure 2

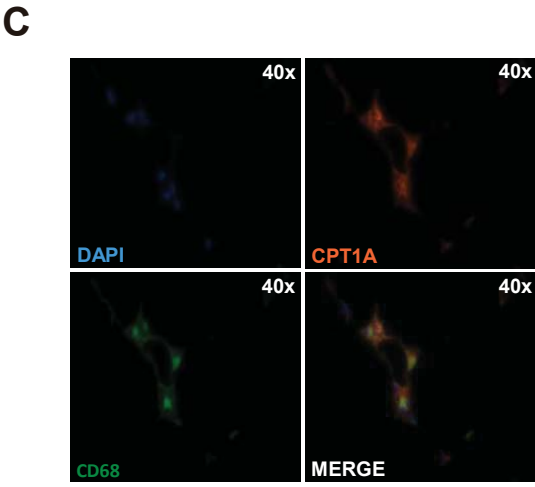
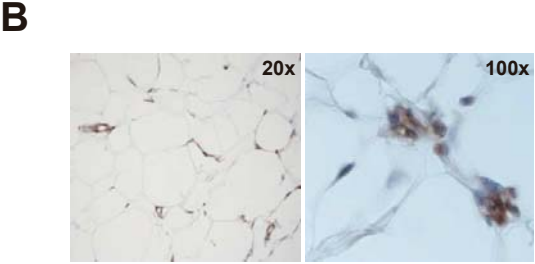
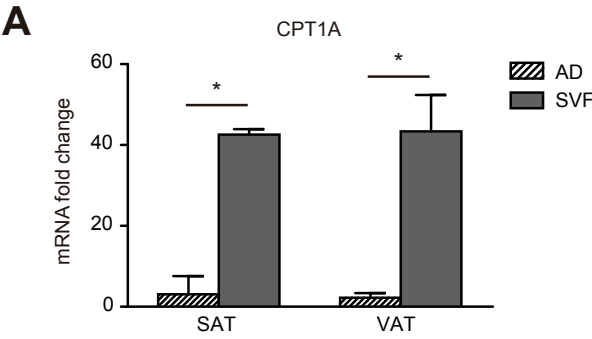


Figure 3

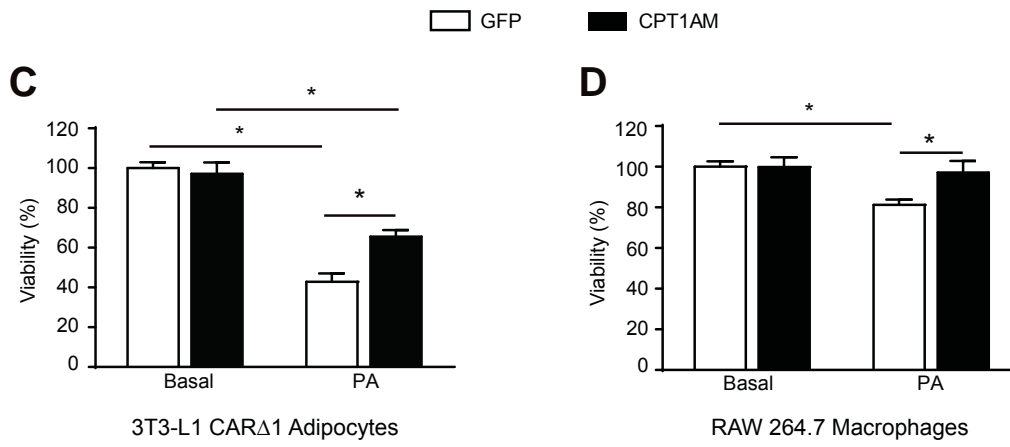
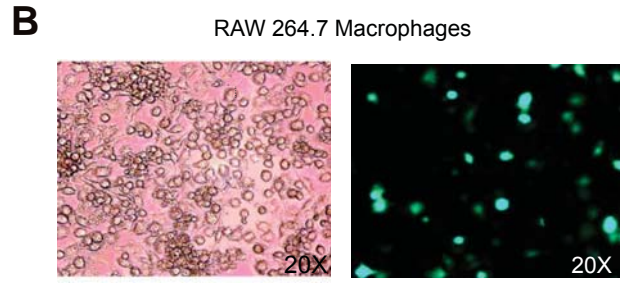
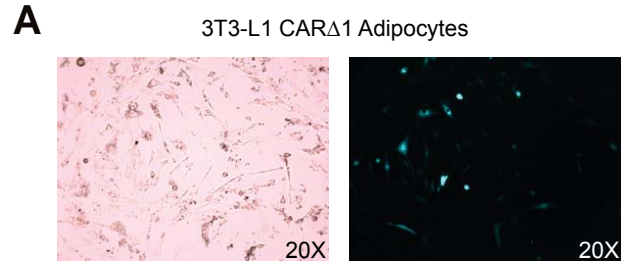


Figure 4

□ GFP ■ CPT1AM

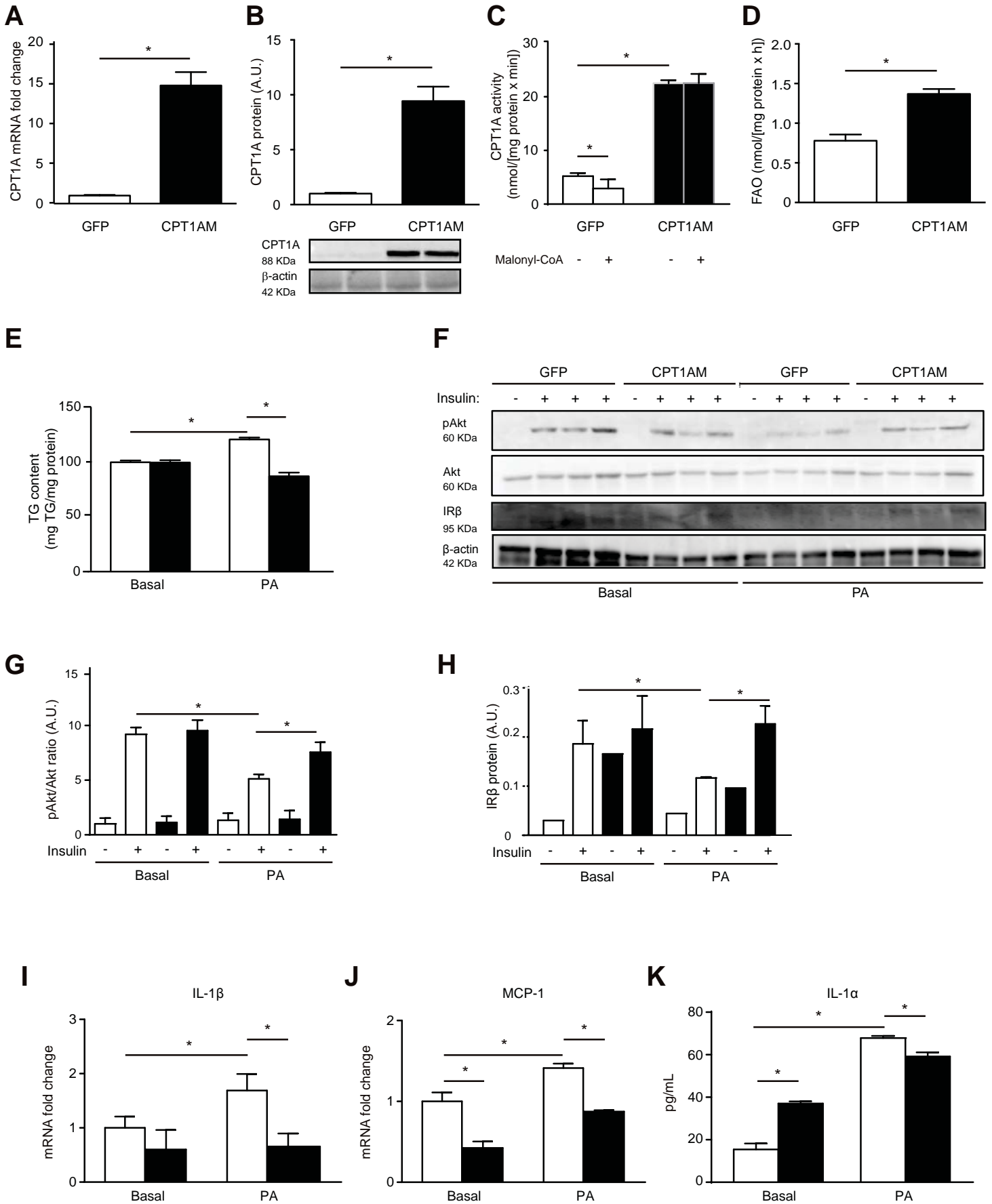


Figure 5

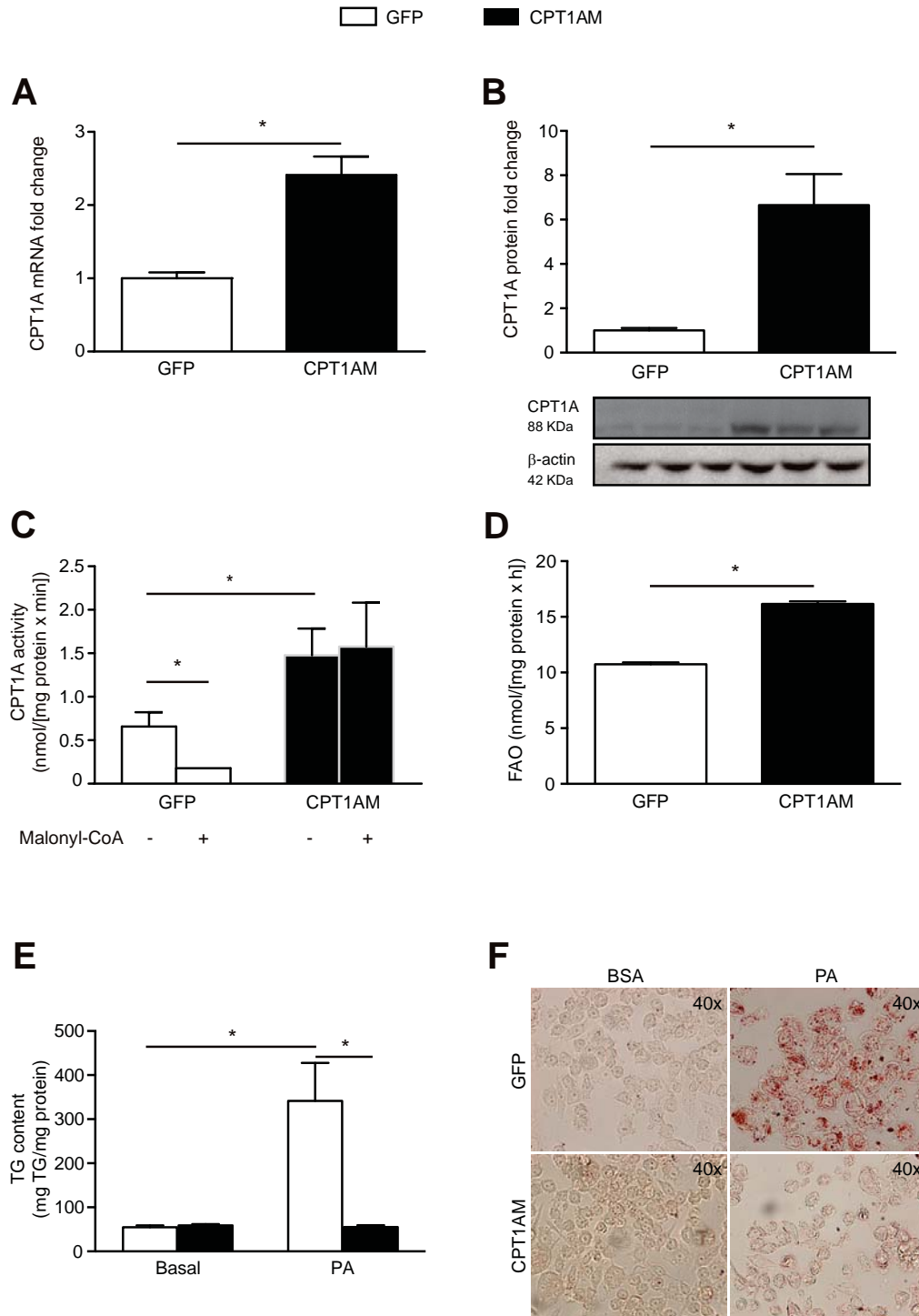


Figure 6

□ GFP ■ CPT1AM

